This full text paper was peer-reviewed at the direction of IEEE Instrumentation and Measurement Society prior to the acceptance and publication.

Magnetic moment direction estimation based on magnetic anomaly signature analysis

Jiazeng Wang
Acoustic Science and Technology Laboratory
Harbin Engineering University
Harbin, China
mytruelike@hrbeu.edu.cn

Ying Shen
Acoustic Science and Technology Laboratory
Harbin Engineering University
Harbin, China
shenying@hrbeu.edu.cn

Junqi Gao
Acoustic Science and Technology Laboratory
Harbin Engineering University
Harbin, China
gaojunqi@hrbeu.edu.cn

Lingsi Sun
Acoustic Science and Technology Laboratory
Harbin Engineering University
Harbin, China
sunlingsi@hrbeu.edu.cn

***Abstract*—In this paper, we proposed a measurement procedure to estimate the magnetic moment orientation (MMO) of an object. As vector magnetic field B_i (i=x, y, z) in each orthogonal direction can be regarded as the superposition of the three basic elements along certain direction. We propose an orthogonal energy ratio (OER) algorithm to infer the MMO by calculating the signal energy distribution along each axis. The first step is to develop a theoretical model and obtain the dipole signature waveforms decomposed of 9 basic elements. The second step is to develop a standard OER database which provides a metric reference to compare with the measured OER. In this standard database, the one having the smallest variance is determined as the estimated MMO. Owing to symmetric property in space, it generally introduces 8 possible solutions. In the last step, an octant determination procedure is applied to select the unique MMO. In particular, the algorithm is independent of changes in CPA (closest path approach) and velocity. Through the complete processing of this algorithm, the target MMO can be estimated precisely with limited errors.**

Keywords—magnetic moment, direction, estimation, magnetic anomaly signature

I. Introduction

Highly-sensitive magnetic sensors are capable to detect small magnetic field distortions induced by a moving magnetic object due to its high magnetic permeability. This technique named as Magnetic Anomaly Detection (MAD) can be used for target detection and localization in the areas of sea mine hunting [1], security checking[2], vehicle parking[3], and subsea cable detection [4].

By analyzing the magnetic anomaly signal, it is desirable to determine whether there are targets and even locate them [5]. Compared with scalar sensors, vector magnetic sensors can obtain more information allowing it to estimate the target moving characteristics, such as motion direction, motion speed, CPA distance and so on [6, 7]. Indeed, the magnetic moment information is always a concern for MAD analysis [8]. The estimation of the unknown magnetic moment is essential for target recognition, which should include both the magnetic moment magnitude and direction. There are some studies on the magnetic moment estimation for a stable AC target [9, 10]. But for MAD target detection, the target is always moving and the magnetic moment remains stable for a period of time. Recent theoretical studies have indicated an effect of coefficient of orthonormal basis function on the target MMO [11, 12]. However, there has been no report so far on the dependence of MMO estimation and the orthonormal basis function.

This letter reports the achievement of using a single magnetic sensor for MMO estimation by orthogonal energy ration algorithm. This work builds on our previous study on interpretation of the magnetic signature waveform to obtain the moving behavior of the concealed target in terms of CPA, velocity and moving direction [6, 13]. These studies fuel a more profound inquiry, how to employ the magnetic fingerprint characteristics to obtain the target MMO information? Here, we present realization of an MMO evaluation method by a single magnetic sensor using orthogonal energy ratio (OER) algorithm.

II. Theoretical Model

A. Magnetic dipole model

According to the magnetic anomaly detection theory, magnetic target can be considered as a magnetic dipole when the measuring distance is at least three times longer than the dimension of the target. A magnetic dipole model is firstly established to analyze the magnetic anomaly signatures as changing the orientations of the magnetic dipole. Based on the classic magnetic dipole model, the induced magnetic field $\vec{B}$ can be described as:

$$B(\vec{M},\vec{r}) = \frac{\mu_0}{4\pi}\left[\frac{3(\vec{M}\cdot\vec{r})\vec{r}}{|\vec{r}|^5} - \frac{\vec{M}}{|\vec{r}|^3}\right] \quad (1)$$

where $\mu_0 = 4\pi \times 10^{-7} H/m$ is the space permeability, $\vec{r} = [x \quad y \quad z]^T$ is the position vector of the magnetic dipole, and $\vec{M} = [M_x \quad M_y \quad M_z]^T$ refers to the magnetic moment vector of

This paper is funded by the International Exchange Program of Harbin Engineering University for Innovation-oriented Talents Cultivation. This work was supported in part by the Natural Science Foundation of Heilongjiang Province of China (LH2019E040) and the Academy of Space Electronic Information Technology (6142411183410). The project was supported by the China Ship Development and Design Center Grant (KY10500190043) and Acoustic Science and Technology Laboratory Grant (JCKYS2019604SSJS005).

978-1-7281-4460-3/20/$31.00 ©2020 IEEE

the target. After bringing $\vec{M}$ and $\vec{r}$ into equation (1), a matrix form can be obtained as the following:

$$\begin{bmatrix} B_x \\ B_y \\ B_z \end{bmatrix} = \frac{\mu_0}{4\pi R^5} \begin{bmatrix} 3x^2 - R^2 & 3xy & 3xz \\ 3xy & 3y^2 - R^2 & 3yz \\ 3xz & 3yz & 3z^2 - R^2 \end{bmatrix} \begin{bmatrix} M_x \\ M_y \\ M_z \end{bmatrix} \quad (2)$$

where $R = |\vec{r}|$ and $[B_x \quad B_y \quad B_z]^T$ are the three components of $\vec{B}$ in each orthogonal direction.

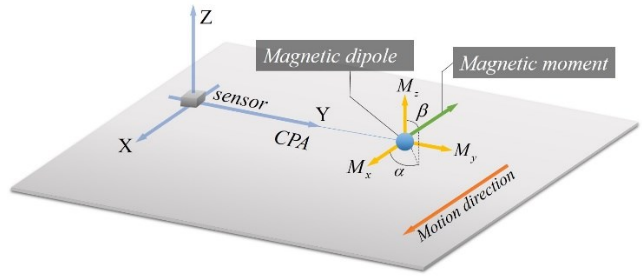

Fig. 1. Schematic diagram of MAD simulation model

Fig. 1 shows the configuration of a magnetic vector sensor and a moving dipole used in this work. The sensor is assigned at the original point of the orthogonal coordinate system. The dipole is set to move along the x-axis within x-y plane at a constant velocity of v with CPA equal to R_0. So the position of the dipole relative to the sensor can be written as:

$$\begin{cases} x = vt \\ y = R_0 \\ z = 0 \end{cases} \quad (3)$$

On the other hand, the orientation of the magnetic moment is defined by the angles α and β in this simulation. α is used to describe the angle between the positive x-axis and projection of the magnetic moment into the x-y plane β is the angle between the magnetic moment and the positive z-axis. Thus, the components of the magnetic moment can be defined as:

$$M_x = \sin\beta \cos\alpha \, |\vec{M}|$$

$$M_y = \sin\beta \sin\alpha \, |\vec{M}|$$

$$M_z = \cos\beta |\vec{M}| \quad (4)$$

Combing equations (3) and (4) into equation (2) that can be expressed as:

$$\begin{bmatrix} B_x(t) \\ B_y(t) \\ B_z(t) \end{bmatrix} = \frac{\mu_0|\vec{M}|}{4\pi R_0^3} \begin{bmatrix} \frac{2(vt/R_0)^2-1}{(1+(vt/R_0)^2)^{5/2}} & \frac{3(vt/R_0)}{(1+(vt/R_0)^2)^{5/2}} & 0 \\ \frac{3(vt/R_0)}{(1+(vt/R_0)^2)^{5/2}} & \frac{2-(vt/R_0)^2}{(1+(vt/R_0)^2)^{5/2}} & 0 \\ 0 & 0 & \frac{-(vt/R_0)^2-1}{(1+(vt/R_0)^2)^{5/2}} \end{bmatrix} \begin{bmatrix} \cos\alpha \sin\beta \\ \sin\alpha \sin\beta \\ \cos\beta \end{bmatrix} \quad (5)$$

In order to simplify equation (5), we define a feature matrix $k(t)$ as:

$$k(t) = \frac{\mu_0|\vec{M}|}{4\pi R_0^3} \begin{bmatrix} \frac{2t^2-1}{(1+t^2)^{5/2}} & \frac{3t}{(1+t^2)^{5/2}} & 0 \\ \frac{3t}{(1+t^2)^{5/2}} & \frac{2-t^2}{(1+t^2)^{5/2}} & 0 \\ 0 & 0 & \frac{-t^2-1}{(1+t^2)^{5/2}} \end{bmatrix} = \begin{bmatrix} k_{x1}(t) & k_{x2}(t) & k_{x3}(t) \\ k_{y1}(t) & k_{y2}(t) & k_{y3}(t) \\ k_{z1}(t) & k_{z2}(t) & k_{z3}(t) \end{bmatrix} \quad (6)$$

Then equation (5) can be rewritten as:

$$\begin{bmatrix} B_x(t) \\ B_y(t) \\ B_z(t) \end{bmatrix} = \begin{bmatrix} k_{x1}(vt/R_0) & k_{x2}(vt/R_0) & k_{x3}(vt/R_0) \\ k_{y1}(vt/R_0) & k_{y2}(vt/R_0) & k_{y3}(vt/R_0) \\ k_{z1}(vt/R_0) & k_{z2}(vt/R_0) & k_{z3}(vt/R_0) \end{bmatrix} \begin{bmatrix} \cos\alpha \sin\beta \\ \sin\alpha \sin\beta \\ \cos\beta \end{bmatrix} \quad (7)$$

Equation (7) can be further decomposed into 9 basic elements:

$$\begin{cases} B_x(t) = B_{x1}(t) + B_{x2}(t) + B_{x3}(t) \\ B_y(t) = B_{y1}(t) + B_{y2}(t) + B_{y3}(t) \\ B_z(t) = B_{z1}(t) + B_{z2}(t) + B_{z3}(t) \end{cases} \quad (8)$$

where

$$\begin{pmatrix} B_{x1}(t) = \cos\alpha \sin\beta \cdot k_{x1}(t) & B_{x2}(t) = \sin\alpha \sin\beta \cdot k_{x2}(t) & B_{x3}(t) = \cos\beta \cdot k_{x3}(t) \\ B_{y1}(t) = \cos\alpha \sin\beta \cdot k_{y1}(t) & B_{y2}(t) = \sin\alpha \sin\beta \cdot k_{y2}(t) & B_{y3}(t) = \cos\beta \cdot k_{y3}(t) \\ B_{z1}(t) = \cos\alpha \sin\beta \cdot k_{z1}(t) & B_{z2}(t) = \sin\alpha \sin\beta \cdot k_{z2}(t) & B_{z3}(t) = \cos\beta \cdot k_{z3}(t) \end{pmatrix} \quad (9)$$

From equation (9), it is clear to see that the obtained signal in one orthogonal direction can be regarded as the superposition of three basic elements under certain direction. As the strength of magnetic moment $|\vec{M}|$ is constant, the orientation of moment defined by angle α and β assigns different weights to each element that governs the waveform distributions. For example, if set $\alpha = 45°$ and $\beta = 30°$, the induced magnetic fields of each element are shown in Fig. 2 when $|\vec{M}| = 1A \cdot m^2$, $v = 1$m/s and CPA=$1m$.

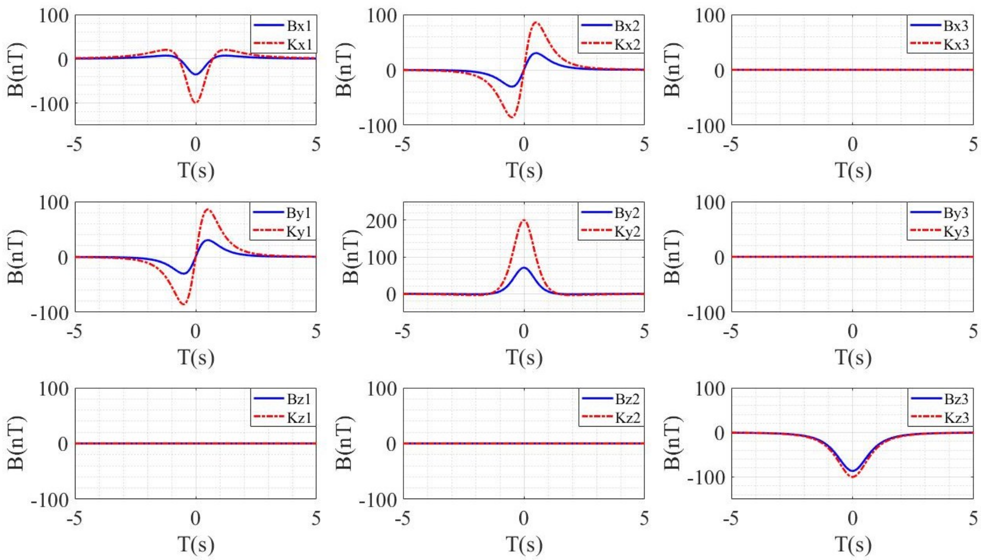

Fig. 2. Waveforms of 9 basic elements as α=45° and β=30°

From equation (6), it can be concluded that the angles α and β have no influence on the k function. It implies that the patterns of k_{ij} (i=x, y, z; j=1, 2, 3) are kept stable, as shown in Fig. 2. The widths and amplitudes of k function waveforms are found to be dependent on the ratio of v/R_0. On the other hand, however, the waveforms of B_{ij} are dependent on the orientation of magnetic moment, which is not always as illustrated in this as shown in Fig. 2. Indeed, the inverse option to employ the induced B_{ij} signature characteristics opens up the possibility to use such waveform configuration for target MMO identification.

B. *Orthogonal energy ratio algorithm*

Based on the simulation results, we propose an orthogonal energy ratio (OER) algorithm to estimate the orientation of magnetic moment. The OER algorithm provides a reliable mathematical approach to determine the maximum likelihood of the target MMO.

Generally, the algorithm contains three steps: first of all, the durations of measured magnetic signals need to be determined. To do that, the parameter T is assigned to describe the signal duration, which is corresponding to the attenuation of the peak total magnetic field B_t. For a 3-axis vector magnetometer, its total magnetic field can be calculated according to the following formula:

$$B_t = \sqrt{{B_x}^2 + {B_y}^2 + {B_z}^2} \tag{10}$$

The second step is to determine the octant of the MMO. Based on the relationships between B_{ij} and k_{ij}, MATLAB is used to calculate the integration of each element in matrix k (equation 6) in arange of -T/2 to T/2 as follows:

$$\int_{-T/2}^{T/2} \frac{B_{x1}(t)}{\cos\alpha \sin\beta} dt = \int_{-T/2}^{T/2} k_{x1}(t)dt < 0 \quad (\cos\alpha \sin\beta \neq 0) \tag{11}$$

$$\int_{-T/2}^{T/2} \frac{B_{y2}(t)}{\sin\alpha \sin\beta} dt = \int_{-T/2}^{T/2} k_{y2}(t)dt > 0 \quad (\sin\alpha \sin\beta \neq 0) \tag{12}$$

$$\int_{-T/2}^{T/2} \frac{B_{z3}(t)}{\cos\beta} dt = \int_{-T/2}^{T/2} k_{z3}(t)dt < 0 \quad (\cos\beta \neq 0) \tag{13}$$

$$\int_{-T/2}^{T/2} B_{x2}(t)dt = \int_{-T/2}^{T/2} B_{y1}(t)dt = 0 \tag{14}$$

Based on equations (11)-(14), the magnetic signals measured by magnetic sensors can be found to have the following characteristics:

$$\int_{-T/2}^{T/2} Bx(t)dt = \int_{-T/2}^{T/2} Bx1(t)dt = \cos\alpha \sin\beta \int_{-T/2}^{T/2} k_{x1}(t)\, dt \tag{15}$$

$$\int_{-T/2}^{T/2} By(t)dt = \int_{-T/2}^{T/2} By2(t)dt = \text{sina}\,\alpha \sin\beta \int_{-T/2}^{T/2} k_{y2}(t)\, dt \tag{16}$$

$$\int_{-T/2}^{T/2} Bz(t)dt = \int_{-T/2}^{T/2} Bz3(t)dt = \cos\beta \int_{-T/2}^{T/2} k_{z3}(t)\, dt \tag{17}$$

In order to simplify the relationships between measured magnetic field $[B_x \quad B_y \quad B_z]^T$ and MMO shown in equations [14-16], a step function h(ε) is used as the following:

$$h(\varepsilon) = \begin{cases} 1 & \varepsilon > 0 \\ 0 & \varepsilon \leq 0 \end{cases} \tag{18}$$

Thus, we can obtain the following equation:

$$h_x = h\left(\int_{-T/2}^{T/2} B_x(t)dt\right) = h(-\cos\alpha \sin\beta) \quad (\cos\alpha \sin\beta \neq 0)$$

$$h_y = h\left(\int_{-T/2}^{T/2} B_y(t)dt\right) = h(\sin\alpha \sin\beta) \quad (\sin\alpha \cos\beta \neq 0)$$

$$h_z = h\left(\int_{-T/2}^{T/2} B_z(t)dt\right) = h(-\cos\beta) \quad (-\cos\beta \neq 0) \tag{19}$$

Then a matrix of H=$[h_x \quad h_y \quad h_z]$ can be used to identify the unique octant in 3-D space of MMO, as shown in Table 1.

TABLE I. INTERVAL SELECTION OF MAGNETIC MOMENT DIRECTION

β \ α	(0°, 90°)	(90°, 180°)	(180°, 270°)	(270°, 360°)
(0°, 90°)	[0 1 0]	[1 1 0]	[1 0 0]	[0 0 0]
(90°, 180°)	[0 1 1]	[1 1 1]	[1 0 1]	[0 0 1]

The final step is to estimate more precise MMO based on the calculation of OER. Analysis in section II. B has indicated that the MMO can affect the waveform distributions. Accordingly, we estimate the MMO through calculating energy distribution of the signals along each axis. In detail, we define the signal energy of each axis within the duration T by the following formula:

$$E_i = \int_T B_i^2(t)dt \quad i = x, y, z \tag{20}$$

In order to make the algorithm more flexible for MAD application, the model does not consider the CPA and the magnitude of magnetic moment. We normalize the energy of signal along each axis to obtain the orthogonal energy ratio. Based on formula (20), the three OERs $[e_x \quad e_y \quad e_z]$ can be defined as:

$$e_i = \frac{E_i}{E_x+E_y+E_z} \quad i = x, y, z \tag{21}$$

Based on equation (21), we build up a standard library for subsequent solutions that represents the orthogonal energy ratio by considering different magnetic moment directions(α, β). The OERs in this standard library are defined as $[S_x(\alpha,\beta) \quad S_y(\alpha,\beta) \quad S_z(\alpha,\beta)]$ in a matrix of 360×180×3. For measured magnetic signals, we scan the standard library under different(α, β), and then calculate the variance between the OER standard library and the measured OER. The one has the smallest variance is determined to be the estimated MMO of the target. The search results are given in a form of ambiguity plane $P(\alpha, \beta)$ as follows:

$$P(\alpha,\beta) = 10\,log \frac{1}{(C_x(\alpha,\beta)-e_x)^2+\left(C_y(\alpha,\beta)-e_y\right)^2+(C_z(\alpha,\beta)-e_z)^2} \tag{22}$$

where e_x, e_y and e_z are the OERs of the signals that need to be estimated. In order to better understand the ambiguity plane, one example is given to show the working principle. The values in standard library are calculated under the conditions of $v = 1$m/s, CPA=1m and $|\vec{M}| = 1$A·m^2. And the signals that need to be estimated is set under the condition of $v = 0.5$m/s, CPA=10m and $|\vec{M}| = 10$A·m^2 when α=30° and β=60°. The typical ambiguity plane is shown in Fig.3

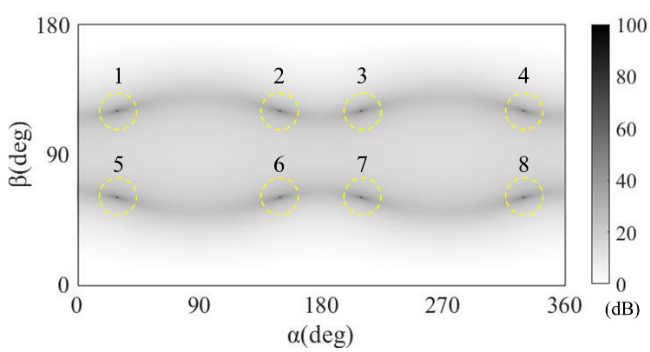

Fig. 3. Magnetic moment direction diagram of OER

Fig. 3 shows that there are 8 possible MMOs based on the third step of the OER algorithm. Because this step only considers the energy intensity of obtained magnetic signals, each octant contains one determined result due to the spatial symmetry. Afterwards, the octant of the true MMO would been determined in step 2. In this case, the final estimated orientation is peak No. 5, which is corresponding to the MMO of α=30° and β=60°. More importantly, the algorithm has been also demonstrated to be independent with parameters of CPA and velocity considering the standard library and simulated signals configured under different conditions. It needs to be noticed that the MMO of the target should be stable during the measurement. Through the complete processing of the algorithm described in this section, the direction of the magnetic moment can be estimated precisely.

III. EXPERIMENTAL DEMONSTRATION

The experimental system is comprised of a highly-sensitive fluxgate magnetometer and a non-magnetic sliding track, as shown in Fig. 4. Main parameters of the fluxgate sensor are shown in Table 2. During measurement, magnetometer was placed at the original point, and the X, Y and Z axes of sensor were aligned with that of the coordinate system shown in Fig. 4. A small permanent magnetic disc with 30mm diameter was used as the target whose magnetic moment was perpendicular to its surface. The magnetic moment direction relative to the coordinate system is changed by adjusting the attitude of the magnetic disc itself. In line with the motion model in Fig.1, the sliding track is used to take the magnetic disc to simulate the uniform linear motion. It should be noticed that a bracket is installed to reduce the electro-magnetic interference of the sliding track.

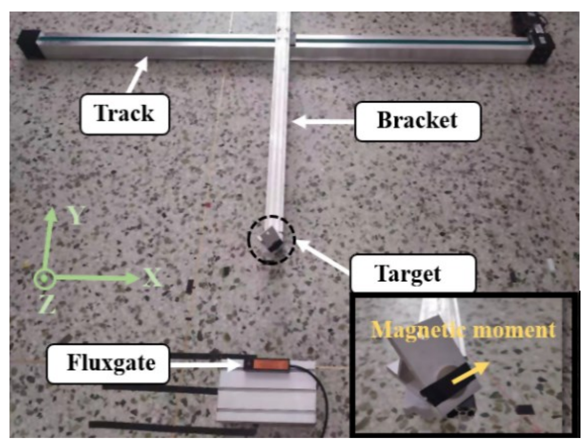

Fig. 4. Experiment setup picture including a 1.8m slide track and a Fluxgate

TABLE II. THE MAIN PARAMETERS OF THREE-AXIS FLUXGATE

Axis	X	Y	Z
Sensitivity (V/Oe)	10.0017	10.0029	10.005
Orthogonality error (Deg)	0.043	0.041	0.085
Self-noise (pT/ √ Hz) [@1Hz]	4.95	5.84	5.64

We collect the target magnetic abnormal signals under different magnetic moment directions and process the data using the proposed OER algorithms. The velocity of the target is 0.3m/s and CPA is 0.2m in the experiment. Then the obtained (B_x, B_y, B_z) data is computed by the proposed OER algorithm, and the estimated MMO angles are shown in Table 3. Notice that good estimation can be achieved under different MMOs in the case of real experiment. Though the experiment results have not been configured to allow for extremely precise determination of MMO, we believe that the errors are in an acceptable range, and supportive for the proposed evaluation method. These experiment results demonstrate that OER method is an enabling technology for MMO determination.

Theoretically, the proposed OER algorithm is an unbiased evaluation approach with respect to symmetrical MMOs. However, the estimated data and errors in Table 3 indicates that the estimation accuracy varies in different octants. Thus, the results suggest that there must be errors arisen from practical measurements.

TABLE III. THE ESTIMATION OF DIFFERENT DIRECTION OF MAGNETIC MOMENT

Real (α, β)	**45°, 45°**	**225°, 135°**	**315°, 135°**	**135°, 45°**
Estimation of OER	50°, 44°	218°, 135°	324°, 138°	131°, 42°

IV. CONCLUSION

In summary, we study the characteristic of magnetic abnormal signals received by a three-axis magnetic sensor and the direct estimation of magnetic moment is analyzed based on this. The abnormal magnetic signal received by the three-axis magnetic sensor can be further decomposed into 9 elements, and the motion velocity v and CPA of the target-related parameters have the same effect on each element. The magnetic moment direction gives different weights to each element to form each axial signal. Based on the above properties, OER algorithms for calculating the direction of the magnetic moment of magnetic objects in uniform motion are proposed in this paper. OER algorithm uses the energy ratio between axial to estimate the direction of the magnetic moment and uses the integral value of the signal to judge the direction interval of the magnetic moment. Simulation and experiment also verify that OER algorithm can predict MMO with good accuracy.

The proposed OER algorithm based on magnetic signature analysis offers robust and low computation-load detection procedure that is vital for successful real-time MAD sensing. Further work will be devoted to analyze the relationship between the moving direction of the target and the characteristics of magnetic abnormal signal.

REFERENCES

[1] G. Sulzberger *et al.*, "Hunting Sea Mines with UUV-Based Magnetic and Electro-Optic Sensors," in *Oceans 2009, Vols 1-3*(Oceans-Ieee, 2009, pp. 1075-1079.

[2] J. Gao, J. Wang, L. Zhang, Q. Yu, Y. Huang, and Y. Shen, "Magnetic Signature Analysis for Smart Security System Based on TMR Magnetic Sensor Array," *IEEE Sensors Journal,* vol. 19, no. 8, pp. 3149-3155, 2019.

[3] P. Nguyen, H. Nguyen, D. Nguyen, T. N. Dinh, H. M. La, and T. Vu, "ParkSense: Automatic Parking Positioning by Leveraging In-Vehicle Magnetic Field Variation," IEEE Access, vol. 5, pp. 25021-25033, 2017.

[4] S. D. Billings, C. Pasion, S. Walker, and L. Beran, "Magnetic models of unexploded ordnance," IEEE Transactions on Geoscience and Remote Sensing, vol. 44, no. 8, pp. 2115-2124, 2006.

[5] Y. Shen et al., "AC magnetic dipole localization by a magnetoelectric sensor," Smart Materials and Structures, vol. 21, no. 6, p. 065007, 2012/05/11 2012.

[6] Y. Shen, J. Wang, J. Shi, S. Zhao, and J. Gao, "Interpretation of signature waveform characteristics for magnetic anomaly detection using tunneling magnetoresistive sensor," Journal of Magnetism and Magnetic Materials, vol. 484, pp. 164-171, 2019/08/15/ 2019.

[7] R. Otnes and Ieee, Static magnetic dipole detection using vector linear prediction, Anderson functions, and block-based adaptive processing (Oceans 2007 - Europe, Vols 1-3). 2007, pp. 532-537.

[8] J. Zhou, J. Chen, and Z. Shan, "Spatial Signature Analysis of Submarine Magnetic Anomaly at Low Altitude," IEEE Transactions on Magnetics, vol. 53, no. 12, pp. 1-7, 2017.

[9] A. Moschitta, A. D. Angelis, F. Santoni, M. Dionigi, P. Carbone, and G. D. Angelis, "Estimation of the Magnetic Dipole Moment of a Coil Using AC Voltage Measurements," IEEE Transactions on Instrumentation and Measurement, vol. 67, no. 10, pp. 2495-2503, 2018.

[10] K. Yamazaki and T. Kawamoto, "Simple estimation of equivalent magnetic dipole moment to characterize ELF magnetic fields generated by electric appliances incorporating harmonics," IEEE Transactions on Electromagnetic Compatibility, vol. 43, no. 2, pp. 240-245, 2001.

[11] B. Ginzburg, L. Frumkis, and B.-Z. Kaplan, "An efficient method for processing scalar magnetic gradiometer signals," Sensors and Actuators A: Physical, vol. 114, no. 1, pp. 73-79, 2004.

[12] B. Ginzburg, L. Frumkis, and B.-Z. Kaplan, "Processing of magnetic scalar gradiometer signals using orthonormalized functions," Sensors and Actuators A: Physical, vol. 102, no. 1, pp. 67-75, 2002/12/01/ 2002.

[13] Y. Shen, D. Hasanyan, J. Gao, Y. Wang, J. Li, and D. Viehland, "A magnetic signature study using magnetoelectric laminate sensors," Smart Materials and Structures, vol. 22, no. 9, p. 095007, 2013/08/01 2013.

[14] D. Liu et al., "Direction identification of a moving ferromagnetic object by magnetic anomaly," Sensors and Actuators A: Physical, vol. 229, pp. 147-153, 2015/06/15/ 2015.

[15] Y. Tang et al., "Detection of Magnetic Anomaly Signal Based on Information Entropy of Differential Signal," IEEE Geoscience and Remote Sensing Letters, vol. 15, no. 4, pp. 512-516, 2018.

[16] X. H. Nie, Z. M. Pan, D. S. Zhang, and W. N. Zhang, "Wavelet-Based Adaptive Detection of Magnetic Anomaly Signal Contaminated by 1/f Noise," Applied Mechanics and Materials, vol. 599-601, pp. 1812-1815, 2014.